NANO LETTERS

Letter

pubs.acs.org/NanoLett

Relevance of the Drag Force during Controlled Translocation of a DNA−Protein Complex through a Glass Nanocapillary

Roman D. Bulushev,[†] Sanjin Marion,[‡] and Aleksandra Radenovic*[,†]

[†]Laboratory of Nanoscale Biology, Institute of Bioengineering, School of Engineering, EPFL, 1015 Lausanne, Switzerland

[‡]Institute of Physics, Bijenicka cesta 46, HR-10000 Zagreb, Croatia

Supporting Information

ABSTRACT: Combination of glass nanocapillaries with optical tweezers allowed us to detect DNA−protein complexes in physiological conditions. In this system, a protein bound to DNA is characterized by a simultaneous change of the force and ionic current signals from the level observed for the bare DNA. Controlled displacement of the protein away from the nanocapillary opening revealed decay in the values of the force and ionic current. Negatively charged proteins EcoRI, RecA, and RNA polymerase formed complexes with DNA that experienced electrophoretic force lower than the bare DNA inside nanocapillaries. Force profiles obtained for DNA-RecA in our system were different than those in the system with nanopores in membranes and optical tweezers. We suggest that such behavior is due to the dominant impact of the drag force comparing to the electrostatic force acting on a DNA−protein complex inside nanocapillaries. We explained our results using a stochastic model taking into account the conical shape of glass nanocapillaries.

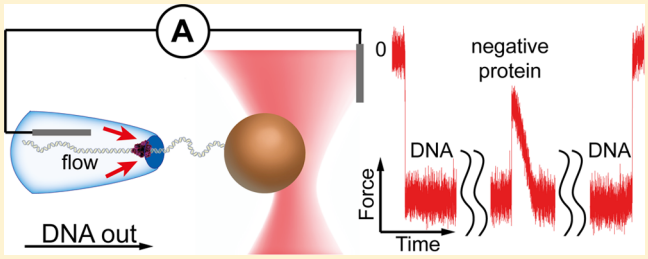

KEYWORDS: *DNA−protein complex, nanocapillary, nanopore, DNA translocation, optical tweezers, force measurements*

Large variety of DNA-binding proteins are constantly involved in numerous processes inside cells in order to maintain a regular cell cycle.[1] Identification and characterization of new proteins responsible for such processes as DNA transcription, replication, recombination, repair, and uptake require knowledge of their DNA-binding properties. Except for traditionally used bulk methods like electrophoretic mobility shift assay (EMSA),[2,3] DNA footprinting,[4] or enzyme-linked immunosorbent assay (ELISA),[5] there are single-molecule techniques allowing for detection of DNA−protein complexes.[6] Among them one can mention fluorescence resonance energy transfer (FRET),[7] optical and magnetic tweezers,[8−11] atomic force microscopy (AFM)[12] and nanopore sensing.[13−23] Single-molecule methods provide additional information regarding unique properties of proteins that cannot be distinguished in bulk experiments. Several excellent examples include estimation of a single-step size of kinesin,[8] direct visualization of backtracking of RNA polymerase on DNA,[24] mechanism of DNA uncoiling by topoisomerase,[25] ATP-induced helicase slippage on DNA,[11] and influence of CpG methylation on stability of a DNA−nucleosome complex.[26] Combination of two single-molecule techniques solid-state nanopores and optical tweezers was performed to controllably translocate a DNA molecule through a nanopore and measure its charge in solution.[27−29] Later it was used to estimate the charge of RNA[30] and detect nucleoprotein filaments[15] and DNA-bound ligands.[18,19]

Glass nanocapillaries are a cheap and easy-to-produce alternative to nanopores in membranes used for various application including detection of DNA,[31,32] proteins,[33,34] and DNA−protein complexes.[23] They can be shrunken under SEM to diameters below 10 nm,[35] providing better signal-to-noise ratio (SNR) in the current signal compared to nanopores in silicon nitride or 2D materials, like graphene.[32,36] In addition, combination of nanocapillaries with optical tweezers does not require a sophisticated microfluidic sample cell and DNA translocation results in a lateral displacement of an optically trapped bead.[37,38] The lateral stiffness of optical tweezers is known to be higher than the axial one, and the measured signals are characterized by better SNR.[39] Recently a combination of nanocapillaries with optical tweezers was used to study mechanism of DNA relaxation[40] and electroosmotic nanojets.[41]

In contrast to nanopores, nanocapillaries have elongated conical shape, so that a potential difference between the cis and trans sides produces a significant electric field within first 100−1000 nm inside the opening.[42] Since the surface charge of nanocapillaries is negative at neutral pH, the electroosmotic flow (EOF) is directed outside of the opening when the positive electrode is in the trans chamber.[41,43,44] In addition, once a DNA molecule is inside a nanopore/nanocapillary the electrophoretic driving force (F_{ep}) on the DNA is reduced due to the EOF-induced drag force (F_{drag}) generated from the flow around its backbone.[42,45] Thus, the total drag opposing

Received: August 14, 2015
Revised: September 13, 2015

DOI: 10.1021/acs.nanolett.5b03264
Nano Lett. XXXX, XXX, XXX−XXX

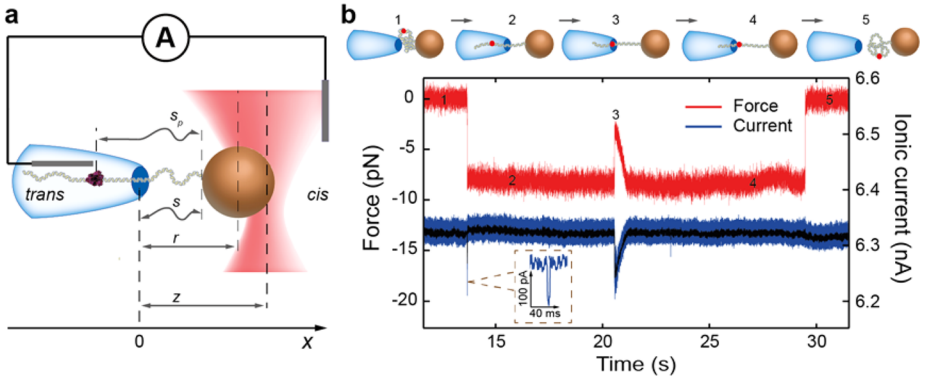

Figure 1. Combination of nanocapillaries and optical tweezers for detection of DNA−protein complexes. (a) Illustration of the setup. An applied electric field initiates DNA translocation through the nanocapillary, whereas the optical tweezers serve as a balance force stalling the DNA inside it. r is the distance from the center of the bead to the opening, z is the distance from the center of the optical trap to the opening, s is the contour length of the DNA, and s_p is the contour length of the DNA until the position of the protein. (b) Measurement of force and current signals during pulling DNA with attached proteins out of a nanocapillary. The cartoon above explains consequent steps of the experiment. The inset shows the current signal corresponding to free translocation of a DNA−protein complex. Afterward this complex was detected during controllable pulling of the DNA molecule out performed with a nanopositioning stage. Thus, it was possible to compare the current signatures of the same attached proteins during free and controlled translocation through the same nanocapillary opening. The amplitude of the conductance drops was similar, whereas the current profiles had different shapes. Movement of the nanopositioning stage initiated after entrance of the DNA molecule with a velocity of 800 nm/s. The experiment was performed with RecA bound proteins in a 44 nm nanocapillary at 150 mV in 150 mM KCl, pH 7.2.

translocation of the DNA is a superposition of flows of counterions originated from negatively charged glass walls and DNA. The electrophoretic force can be interpreted as the bare DNA linear charge density λ_0 being reduced by some value λ_{drag}, resulting in $F_{ep} = (\lambda_0 - \lambda_{drag})\Delta\Phi$, where $\Delta\Phi$ is the potential difference between cis and trans electrodes.

In this Letter for the first time, we used glass nanocapillaries combined with optical tweezers to detect DNA-bound proteins and demonstrate influence of the drag force acting on them inside nanocapillaries. In comparison to free translocation, addition of optical tweezers allows to stall a DNA molecule inside a nanocapillary, controllably pull the DNA outside, and measure the force acting on the DNA and DNA−protein complex. In addition to the force signals we present current signatures of DNA-bound proteins, providing additional information about the studied system. In glass nanocapillaries all detected DNA−protein complexes behaved as if they were less negatively charged than DNA. The electrophoretic force acting on RecA-coated DNA inside nanocapillaries was smaller than on the bare DNA and differed from the results previously obtained in nanopores.[15,18,19] We proposed an explanation of these results based on the EOF-induced drag force. We modified a stochastic model from ref 19 by adapting it to the specific geometry of nanocapillaries to obtain the effective charge of DNA−protein complexes.

Experimental Setup. The setup used in this work combines nanocapillaries and optical tweezers (Figure 1 a).[42] Using the optical tweezers the surface of a polystyrene bead coated with DNA−protein complexes was positioned 2−4 μm away from the nanocapillary opening. The DNA molecules were driven inside the nanocapillary by the electric field. Insertion of a single DNA molecule was confirmed by a simultaneous change in the force and current signals (Figure 1b). The force measured in the system is proportional to the displacement of the optically trapped bead from its equilibrium position $F_{ot} = k(z - r)$, where k is the spring constant of the optical tweezers. After stalling a DNA molecule, the nanocapillary was moved away from the optically trapped bead using a nanopositioning stage until the DNA molecule was completely pulled out, e.g., force and current signals restored to the initial levels (Figure 1b). At the position corresponding to the protein attached to the DNA a sudden change in the force and current traces was observed followed up by their decay, while the nanocapillary was moved further away (Figure 1b).

Theoretical Model. In the system combining nanocapillaries and optical tweezers the electrophoretic force (F_{ep}) pulling DNA inside the nanocapillary is balanced by the harmonic restoring force of the optical tweezers (F_{ot}). These two forces act to extend the DNA, whereas the entropic force (polymer extension) of DNA opposes them. The force on the bead exerted by the optical tweezers is equal to the electrophoretic force ($F_{ot} = F_{ep}$), except when additional forces are introduced, i.e., the force on a DNA−protein complex during its translocation.

The system was modeled with a pair of coupled Langevin equations for two state variables,[19] including the distance r of the bead center from the opening and the contour length of DNA s from the bead to the opening (Figure 1 a). The evolution of the state variables is governed by the free energy of the system:

$$G(r, s) = G_{DNA}(s) + G_{wlc}(r, s) + G_{ot}(r) + G_p(s) \quad (1)$$

with contributions from the optical trap $G_{ot}(r) = 1/2k(z - r)^2$, where $G_{wlc}(r,s)$ is the entropic free energy of a worm like chain of DNA, $G_{DNA}(s)$ is the free energy of a charged DNA molecule in the nanocapillary, and $G_p(s)$ is the free energy contribution from a protein bound to the DNA at the position s_p (see section S2 of SI). The two Langevin equations were coupled by the DNA spring free energy $G_{wlc}(r,s)$, which depends on both state variables r and s.

We applied the stochastic model in the geometry of a nanocapillary extracted from images obtained with scanning electron microscope (SEM). Shrinking of a nanocapillary under SEM changes the shape of the tip to the geometry approximated by two truncated cones (Figure S1), where T and t are the taper lengths of large and small cones, respectively, β and α are the opening angles of large and

DOI: 10.1021/acs.nanolett.5b03264
Nano Lett. XXXX, XXX, XXX−XXX

small cones, respectively, and R_0 is the radii of the opening. Applying the continuity condition for the electric field and potential inside two cones, the electrostatic potential inside the small cone can be expressed as

$$V_1(x) = \Delta\Phi \frac{Ax}{\left(1 - \frac{x}{\xi}\right)\xi} + \Delta\Phi \quad (2)$$

and inside the large cone:

$$V_2(x) = \Delta\Phi \frac{B}{1 - \frac{x+t}{\zeta}} \quad (3)$$

Here $\xi = d/(2\tan\alpha)$ and $\zeta = D/(2\tan\beta)$ are the electrostatic potential decay lengths, and A and B are the constants dependent on ξ, ζ, and t (see section S2 of SI).

Knowing the potential, we can calculate the free energy of DNA and DNA−protein complexes and consequently extract forces acting on them. The total force on a DNA-bound protein (F_p) is a combination of the electrostatic force (F_{el}) and the drag force (F_{dr}). F_{el} depends on the charge of the complex and F_{drag} on its size and shape. The balance of these two forces mediated by the DNA worm like chain gives the characteristic force profiles for DNA−protein complexes shown in Figure 1b.

In order to quantify the impact of the EOF in F_p we used numerical simulations in COMSOL Multiphysics. We modeled the system using the Poisson−Nernst−Planck−Stokes equations in the geometry of a nanocapillary (see section S3 of SI, Figure S1). A DNA−protein complex was modeled as a charged rod with a sphere with different charge density coaxial to the nanocapillary (Figure S4). The force on the protein originated from the fluid flow was calculated using a COMSOL built-in reaction force function for different distances x of the protein from the nanocapillary opening (Figure S4). From the simulations we concluded that the EOF-induced drag force on the proteins is well-approximated by the Stokes drag equation $F_{stokes} \sim R_p u\eta$, where R_p is the protein hydrodynamic radii, u is the fluid velocity, and η is the dynamic viscosity. For the general geometry used in the model the drag force can be as high as several pN, e.g., sufficient to significantly influence the total force on the protein F_p. The EOF-induced drag force will consequently renormalize the real value of the charge of a DNA−protein complex.

Detection of DNA-Bound Proteins with Nanocapillaries and Optical Tweezers. In our system we studied three proteins EcoRI, RecA, and RNA polymerase (RNAP) with different physical-chemical characteristics (Table 1). In addition, chosen proteins differ in their way of interaction with DNA. EcoRI binds to the DNA as a dimer, RecA forms long polymeric fibers, and RNAP interacts with the DNA as a single protein. While RecA binds nonspecifically to the DNA, EcoRI and RNAP recognize and interact with specific sequences. It is worth mentioning that the complex of EcoRI and RecA with the DNA was previously detected in the system combining nanopores in membranes and optical tweezers, and the choice of such proteins allowed us to directly compare the impact of the geometry of nanocapillaries on the force profiles of the DNA-bound proteins.[19]

Table 1. Proteins Used in This Work with Their Isoelectric Points and Sizes of Corresponding DNA Complexes

protein	diameter of DNA−protein (nm)	isoelectric point (pI)
EcoRI	≈5[12]	≈6.4[46]
RNAP	≈10[47]	≈5.3[48]
RecA	≈7[16]	≈5.6[16]

Detection of a DNA-EcoRI Complex. EcoRI is a restriction enzyme that is known to cut DNA at the specific sequence GAATTC.[49] However, in the absence of Mg^{2+} ions EcoRI forms a stable complex with DNA without cleaving it.[50−52] After insertion of a single DNA molecule with attached EcoRI inside a nanocapillary, the DNA was pulled out through the opening until the specific peaks in force and current signals corresponding to the DNA−protein complex were revealed (Figure 2b,c). Experiments with DNA-EcoRI complexes were performed in different nanocapillaries and under various buffer conditions with the concentration of KCl 40−400 mM and pH 7.5−8.7 (Table S1, Figure S5). The same EcoRI protein was detected at different potentials applied across the nanocapillary opening (Figure 2d). In general, the measured force on a DNA-EcoRI complex was lower than the one on the bare DNA, and it linearly dependent on the voltage (Figure 2e). At higher potentials the surface area under the protein force curve linearly increased, corresponding to higher work required to pull the DNA−protein complex outside of the nanocapillary. Protein force signatures and their dependence on the voltage were similar to the results obtained with nanopores combined with optical tweezers.[19]

The experimental data were fit to the stochastic model taking into account the specific geometry of a nanocapillary (Figure 2b, Figure S1). The effective charge q of a DNA-EcoRI complex was estimated to be +10−30 e in 40−400 mM KCl, pH 7.5−8.7, which is in the range of the values obtained in ref 19 in 20 mM KCl, pH 8.0.

A DNA-EcoRI complex that is locally positively charged is subject to an additional force F_p directed outside of the nanocapillary (Figure 3). If the electric force on a DNA strand $F_{ep} = \lambda\Delta\Phi$ is comparable to the force F_p exerted on the DNA−protein complex, it will be energetically more favorable for the protein to abruptly displace (jump) to a position where it experiences lower total force. A positively charged complex will jump outside of the nanocapillary (work gain), whereas the jump of a negatively charged complex will be oppositely directed (work investment) in accordance with the orientation of the electrostatic force (Figure S2). Moreover, this jump will cause an abrupt change of the DNA entropic force and thus the DNA contour length s outside of the nanocapillary (Figure S2). The restoration of the force signal to the level observed for the DNA depends on how fast the DNA extension returns to the value before the jump. Pulling DNA-EcoRI back and forth through a nanocapillary opening revealed a hysteresis in the force profiles of ≈8 kT at 200 mV (Figure S6). We attribute this value to an energy barrier for a jump from the cis to the trans state.

The current signature of a DNA-EcoRI complex (Figure 2c) shows a similarity to the force profile as both are related to the position $s-s_p$ of the protein inside the nanocapillary. To detect the current signature of EcoRI we increased the concentration of charge carriers to get 400 mM KCl, providing better SNR. However, we did not detect many DNA−protein complexes in such conditions due to their probable denaturation. We cannot make a conclusion on the direction of the conductance change; however, the event demonstrated in Figure 2c had an increase in the conductance.

DOI: 10.1021/acs.nanolett.5b03264
Nano Lett. XXXX, XXX, XXX−XXX

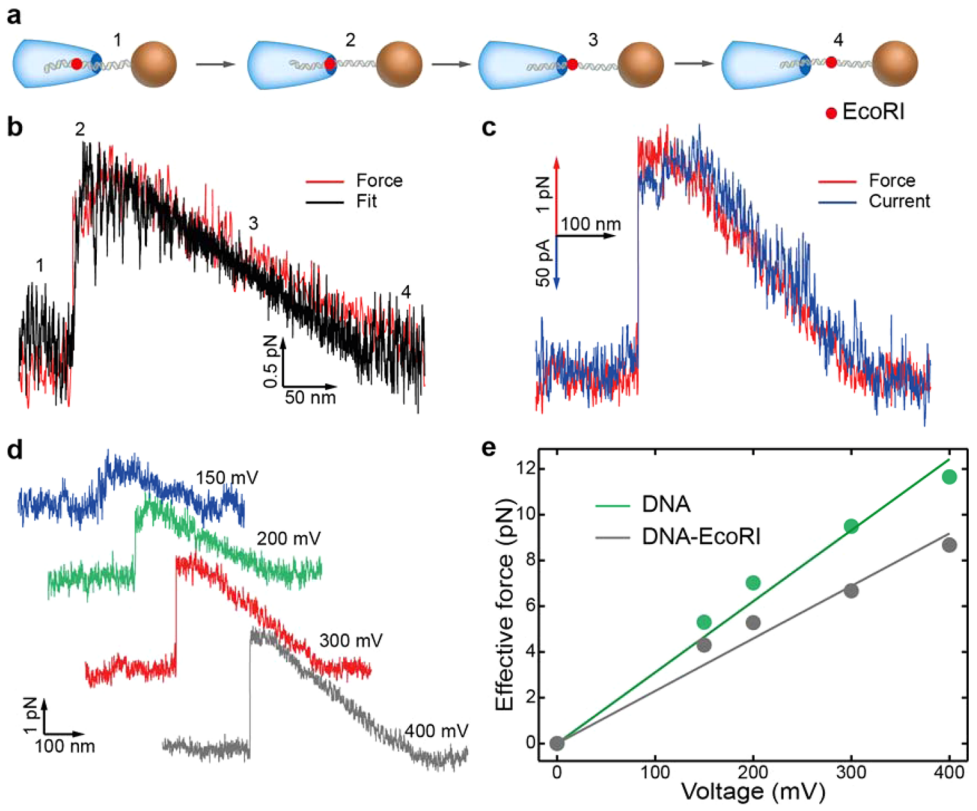

Figure 2. Detection of a DNA-EcoRI complex with glass nanocapillaries and optical tweezers. (a) The cartoon represents the consequent steps of the experiment, where a red circle is an EcoRI protein. The orientation of the nanocapillary used in all experiments presented in this figure was the same as shown here. (b) Force profile of an EcoRI protein bound to DNA (red curve) and its fit to the analytical model (black curve) obtained at 200 mV. (c) Force (red curve) and current (blue curve) signals detected for the same EcoRI at 300 mV. (d) Force profiles of a DNA-EcoRI complex recorded at different voltages. (e) Comparison of the effective force acting on DNA and DNA-EcoRI complex at different voltages. In the case of the complex, the force was measured at the peak maximum, and data were fit to a linear function. All data in this figure were acquired in a 42 nm nanocapillary in 400 mM KCl, pH 8.1.

Detection of DNA-RecA and DNA-RNAP Complexes. Next we studied a DNA-RecA complex, also previously detected in the system with nanopores and optical tweezers.[15,19] This protein plays a key role in recombination, DNA repair, and UV-induced mutagenesis in bacteria.[53] In the presence of ATPγS disassembly of RecA from DNA is drastically decreased resulting in a stable nucleoprotein complex.[54] Due to positive cooperativity RecA forms long filaments on DNA extended by 50% comparing to the DNA molecule.[16] The linear charge density of such filaments is approximately twice higher than those for the bare DNA.[15] In accordance with theory, the electrophoretic force on RecA-coated DNA inside nanopores and measured with optical tweezers was 2−4 times higher compared to the DNA.[15] In addition, force profiles of local RecA structures on the DNA in nanopores exhibited different behavior than for an EcoRI protein due to the different charge of the complex.[19]

However, in glass nanocapillaries DNA-RecA filaments experienced higher electrophoretic force than the bare DNA (Figure 4 a) in 40 mM KCl, pH 7.2−9.0 (Table S1). To perform experiments we first introduced DNA-coated beads in the cis chamber, and the force acting on the bare DNA inside nanocapillaries was recorded. Afterward the chamber was flushed, and beads covered with DNA-RecA were used. The theoretical coverage ratio of the DNA with RecA was 100%; however, we almost never observed fully covered DNA entering nanocapillaries. We assume that the observation of patches of bare DNA is due to low kinetics of RecA polymerization at neutral pH[55] and high stiffness of the nucleoprotein filaments (persistence length ≈950 nm[16]), which could complicate their threading. Indeed, using atomic force microscopy (AFM) we observed stiff DNA-RecA filaments not always fully coated with RecA (Figure S7). In our system a more flexible end of DNA not covered with RecA usually entered the nanocapillary first in accordance with ref 17 (Figure S8).

In order to investigate local RecA structures on DNA, we used the theoretical ratio of RecA to DNA that allows covering 20−60% of the DNA molecule. We detected different segments of RecA on the DNA—long filaments and separate patches (Figure 4c). The electrophoretic force acting on such structures was lower than the one on the bare DNA, which is different from the results obtained in nanopores in membranes.[19]

Comparison of the experimentally obtained curve in Figure 4b with the stochastic model showed that the RecA segment has a length of 1850 nm with an effective linear charge density λ of −0.03 e/nm. Since λ of DNA was −0.15 e/nm in this experiment, RecA forms a complex with the DNA that causes a reduction in its effective linear charge density. As a consequence, such a complex produces a jump characteristic for positively charged proteins from the trans to the cis direction (Figure 4b). These results contradict to the fact that DNA-RecA complexes have higher linear charge density than DNA and lead us to the conclusion that the electrophoretic

DOI: 10.1021/acs.nanolett.5b03264
Nano Lett. XXXX, XXX, XXX−XXX

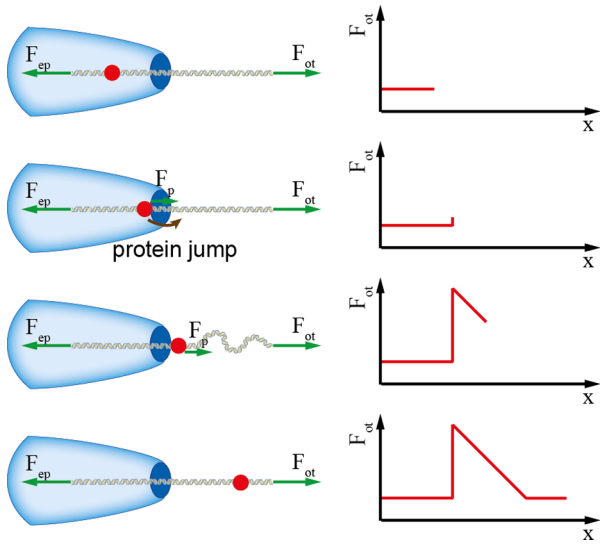

Figure 3. Illustration of a positively charged DNA−protein complex passing through a nanocapillary opening. Cartoons on the left represent consequent steps of the experiment, whereas graphs on the right demonstrate corresponding force signals measured in the system. F_{ot} is the force measured with optical tweezers, F_{ep} is the electrophoretic force acting on the DNA, and F_p is the force acting on the protein. The red circle represents a protein with a positive effective charge. Once such a protein is approached to the nanocapillary opening additional force F_p causes its "jump" to the lowest-energy state. This fast displacement can be observed by the change in the force signal and results in relaxation of the DNA outside of the nanocapillary.

driving force inside nanocapillaries cannot be based only on electrostatic interactions.

To eliminate the possibility of RecA fiber structures influence the measured force, we also studied a complex of a single RNA polymerase (RNAP) with DNA. RNAP is responsible for DNA transcription using nucleoside triphosphates (NTP). In the absence of one of NTPs, it forms a paused transcription complex on the DNA.[56,57] Although the charge of RNAP was estimated to be negative, i.e., equal to −77 e at pH 7.0,[20] we found that a DNA-RNAP complex also reduces the effective local charge of the DNA (Figure 4d). Using the stochastic model, we estimated the effective charge of the DNA-RNAP complex to be +10 e at 40 mM KCl, pH 8.1. In the same experiment λ of the DNA was −0.06 e/nm. Notably, different experimental conditions (buffers and nanocapillaries) cause different linear charge density of DNA due to the difference in the drag force. Considering that RNAP covers a length of DNA of ≈10 nm leads us to a local linear charge density of the complex +0.94 e/nm. Thus, the effective charge of the DNA-RNAP complex is locally positive inside nanocapillaries.

Discussion of Force Profiles of DNA−Protein Complexes. In the system combining nanocapillaries and optical tweezers we observed that negatively charged proteins bound to DNA experience lower electrophoretic force than the bare DNA. In the previous experiments with nanopores and optical tweezers, it was shown that the electrophoretic force on a DNA-RecA complex was higher than on the DNA and opposite for a DNA-EcoRI complex.[15,19] We proposed an explanation of this phenomenon based on the high impact of the drag force during controlled translocation of a DNA−protein complex through a glass nanocapillary.

Nanocapillaries in comparison to nanopores have larger characteristic length where the electrostatic force is enclosed.[42] Based on their shape, nanocapillaries should have a better-formed flow profile, which is known to be directed outward from the opening, opposing the electrostatic force on negatively charged molecules and producing additional drag.[41,43,44] From the other hand, larger penetration of the potential drop inside nanocapillaries leads to the local extension of DNA up to 20−30 persistence lengths inside the nanocapillary compared to just one persistence length inside nanopores (see section S3 of SI). Longer rod-like DNA could also influence better flow formation, resulting in higher drag force. Experimentally this drag can be seen in a 2−5 times smaller effective electrophoretic force on DNA in nanocapillaries than in nanopores.[42,45,58,59]

Another argument supporting the strong impact of the EOF inside nanocapillaries is the difference in the drag force acting on proteins of different sizes. All proteins we used are negatively charged; some are expected to be even more charged than DNA. However, we observed that the linear charge density of RecA is less than those for DNA and that the charge density of RNAP even changes the sign. We attribute this fact to the EOF-induced drag force, which renormalizes the electrostatic charge of the proteins. Based on the sizes of studied DNA−protein complexes (Table 1), we expect RNAP to be subject to the largest drag force and EcoRI − the smallest in identical experimental conditions. From the COMSOL model we concluded that F_{drag} on proteins attached to DNA could be approximated using the Stokes drag equation (see section S3 of SI). Thus, we can relate the ratio of the Stokes drag between these three individual proteins as F_{stokes} (EcoRI): F_{stokes} (RecA): F_{stokes} (RNAP) = 5:7:10. Based on the flow velocity being ∼10 mm/s (Figure S4a), we can estimate that the drag force on these proteins can be above several pN, e.g., sufficient to overcome the electrostatic force.

To additionally support the hypothesis of importance of the drag force in nanocapillaries, we studied free translocation of DNA-RecA complexes. It was previously reported that the force measured with optical tweezers and velocity of translocation are roughly proportional.[45,60] In solid-state nanopores 20% RecA-coated λ-DNA had similar dwell times as the bare DNA.[17] However, in glass nanocapillaries we observed that there was a population of events of partially coated DNA with RecA that had much longer dwell times than the bare DNA (Figure S9). This is consistent with the smaller electrophoretic force acting on the nucleoprotein filaments originated from higher drag force.

Discussion of Conductance Drops of DNA−Protein Complexes. During DNA translocation through a nanopore, the measured conductance can either increase or decrease, depending on the salt concentration.[60] It was considered that at low salt concentrations (<300 mM KCl) DNA enhances the local concentration of charge carriers due to its counterions and produces an increase in the conductance.[60] While at high salt concentrations (>300 mM KCl), a decrease in the conductance was explained as coming from the reduction of the effective cross sectional area available for conduction (a current blockage).[61,62] However, the recent work implies that at all salt concentrations DNA enhances the concentration of local charge carrier and the current blockage model is not applicable.[63] The crossover point at 300 mM KCl is attributed to the dominant frictional forces between the ions and DNA, causing a current drop.[63] In our case, both DNA and protein

DOI: 10.1021/acs.nanolett.5b03264
Nano Lett. XXXX, XXX, XXX−XXX

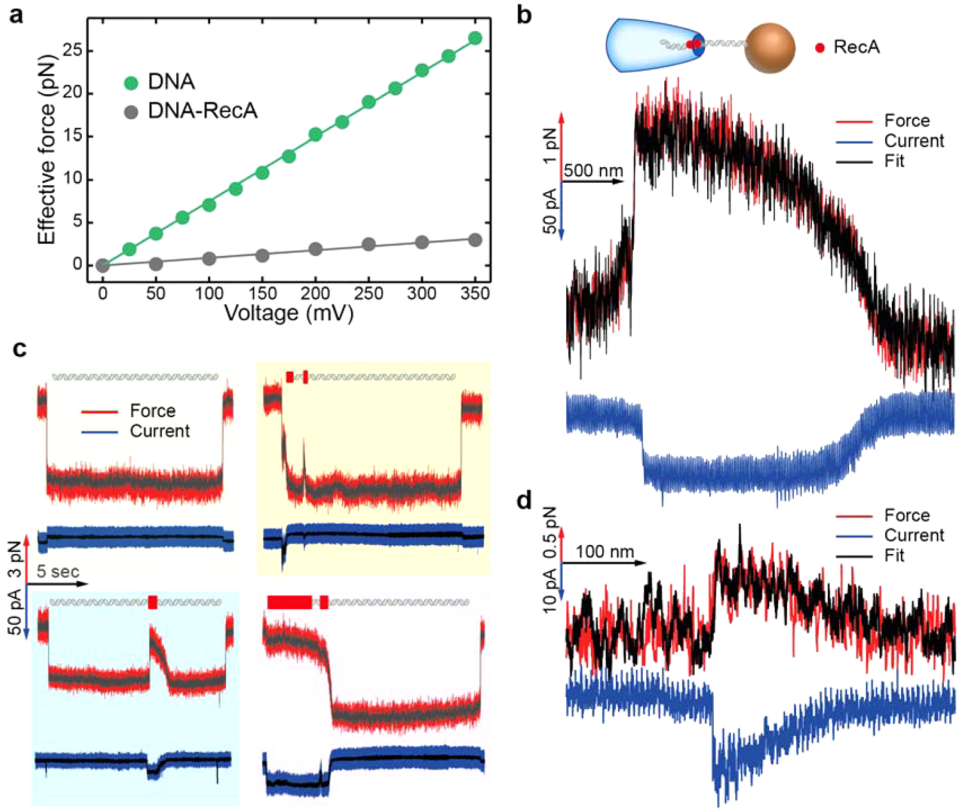

Figure 4. Detection of DNA-RecA and DNA-RNAP complexes with glass nanocapillaries and optical tweezers. (a) Measured force versus voltage acting on DNA and DNA-RecA. The studied fragment of DNA-RecA experienced constant force at least during 500 nm. Data were acquired in a 21 nm nanocapillary in 150 mM KCl, pH 7.5, and fit to a linear function. (b) Force and current signals corresponding to a local RecA structure on DNA, where the red curve is the force signal, the blue curve is the current signal, and the black curve is the fit to the model. The cartoon illustrates the orientation of the nanocapillary used in all experiments presented in this figure. Data were acquired in a 108 nm nanocapillary at 150 mV in 150 mM KCl, pH 7.2. (c) Force and current signals corresponding to DNA and DNA partially covered with RecA, where the red curve is the force signal and the blue curve is the current signal. The red rectangles on the DNA above the graphs correspond to local structures of RecA. The data were acquired in two different 59 nm nanocapillaries at 100 mV (left bottom graph) and 150 mV (all other graphs) in 150 mM KCl, pH 7.2. (d) Force and current profiles of a DNA-RNAP complex, where the red curve is the force signal, the blue curve is the current signal, and the black curve is the fit to the model. The data were acquired in a 44 nm nanocapillary at 150 mV in 40 mM KCl, pH 8.1.

present microscopically rough surfaces and influence the current modulation.

To date, there are not many results of detection of DNA−protein complexes in nanopores/nanocapillaries at low salt concentrations. Usually nanopore experiments are performed in denaturing conditions allowing for detecting only proteins stably bound to DNA.[15,20,21,64] In our system we detected current signatures of DNA−protein complexes in physiological conditions with the concentration of KCl in the range of 40−150 mM (Figure 4b,c,d). Notably, the current in addition to the force signal increases the resolution for detection of local protein structures on DNA, especially in nanocapillaries of small diameters (Figure S8). Current and force signals have similar shapes since they both are related to the position of the protein in respect to the narrowest part of the nanocapillary (Figure 2c, Figure 4b,c,d).

However, to detect current signatures of a DNA-EcoRI complex, we had to increase the concentration to 400 mM KCl. At these nonphysiological conditions, we did not detect many complexes and were not able to make a conclusion regarding the current profile of DNA-EcoRI. In contrast, for DNA-RNAP and DNA-RecA complexes in the range of 40−150 mM KCl, we measured a decrease in the conductance during their controlled translocation (Figure 4b,c,d, Table S1). Our results are different from those obtained for DNA-RecA in the system combining nanopores and optical tweezers, where a conductance drop at 600 mM KCl and a conductance increase at 100 mM KCl were obtained.[15] Comparing these data for DNA-RecA conductance modulation to well-known results for DNA,[60] we would also expect a transition point in the conductance in nanocapillaries. As DNA-RecA has a larger diameter than DNA, we could argue that the molecular friction contribution between charge carriers and RecA surface is stronger at larger drag forces, thus more likely reducing the transition point below our experimental range (<40 mM KCl).[63]

DNA-RNAP conductance drops can be attributed both to a current blockage[62] and to reduction of the current at the surface due to molecular friction,[63] depending on its charge. In the context of our experiments, RNAP has low surface charge density, as the drag force is capable to overcome its electrostatic charge. It is even possible that the drop in the conductance happens due to the fact that a DNA-RNAP complex removes the local DNA counterion charge and thus reduces the number of charge carriers. A similar current drop was detected for a single DNA-2-CysPrx complex during its controlled translocation through nanopores in 20 mM KCl.[18] In our system, it is possible that the EOF contributes to the change of the

DOI: 10.1021/acs.nanolett.5b03264
Nano Lett. XXXX, XXX, XXX−XXX

conductance during translocation of a DNA−protein complex by changing the advective current density[63]—an effect analogous to current polarization.[43] This phenomenon would also explain a conductance drop for RecA-coated DNA that we observed in nanocapillaries at salt concentration as low as 40 mM KCl.

Conclusions. We demonstrated that glass nanocapillaries combined with optical tweezers is a suitable tool for detection of DNA-bound proteins in physiological conditions. Nanocapillaries showed versatility due to their simple fabrication process and high SNR, allowing for the recording of current signatures of DNA−protein complexes. We observed renormalized effective charge of proteins attached to DNA inside nanocapillaries that we attributed to the EOF-induced drag force. The impact of the drag force during translocation of molecules was demonstrated before in nanopores in membranes.[27,45,58,59] In certain cases the drag force dominated the electrostatic force resulting in translocation of charged molecules in the direction against the electric field.[65] On the example of DNA−protein complexes we showed relevance of the drag force during its translocation through conical nanopores made in glass and estimated the drag force to be higher than in nanopores in membranes. One of the possible outlooks of the work would be measurement of the charge of DNA-bound proteins after elimination/reduction of the EOF by making nanocapillary walls neutrally charged, for example by coating them with lipids.[66,67] In the future, such a system can be used to localize different ligands along a DNA molecule and estimate their size based on the current signatures as well as their charge knowing the impact of the drag force. As a consequence this technique opens up the possibility for single-molecule-based mapping of genomes in solution.

■ ASSOCIATED CONTENT

Supporting Information

The Supporting Information is available free of charge on the ACS Publications website at DOI: 10.1021/acs.nanolett.5b03264.

Materials and methods, description and figures of the stochastic model, description and figures of the COMSOL model, figures showing force profiles of complexes of EcoRI and RecA with DNA, a figure showing pulling of a DNA-EcoRI back and forth through the nanocapillary, a figure with AFM images of DNA-RecA complexes, a figure demonstrating consequent translocation of DNA, RecA, and DNA-RecA through a glass nanocapillary (PDF)

■ AUTHOR INFORMATION

Corresponding Author

*E-mail: aleksandra.radenovic@epfl.ch.

Notes

The authors declare no competing financial interest.

■ ACKNOWLEDGMENTS

The authors would like to thank C. Santschi and O. Martin for providing a pipet puller, Center of Micro/Nanotechnology (CMI) EPFL for access to SEM. Falvio Mor, Michael Graf, Tomislav Vuletic, Lely Feletti, Melanie Blokesch, and Lorenz Steinbock for fruitful scientific discussion and technical support. The work was financially supported by the European Research Council (grant no. 259398, PorABEL: Nanopore integrated nanoelectrodes for biomolecular manipulation and design) and FNS (grant no. 200021_153653, Glass nanopores as a versatile tool for single molecule analysis). S. Marion was supported by the "Unity through Knowledge" Fund, Croatia under Grant 17/13 "Confined DNA".

■ REFERENCES

(1) Alberts, B.; Johnson, A.; Julian, L.; Morgan, D.; Raff, M.; Roberts, K.; Walter, P. *Molecular Biology of the Cell*; Routledge: Florence, KY, 2014; p 1464.
(2) Garner, M. M.; Revzin, A. *Trends Biochem. Sci.* **1986**, *11* (10), 395−396.
(3) Hellman, L. M.; Fried, M. G. *Nat. Protoc.* **2007**, *2* (8), 1849−61.
(4) Tullius, T. D. *Annu. Rev. Biophys. Biophys. Chem.* **1989**, *18*, 213−37.
(5) Brand, L. H.; Henneges, C.; Schussler, A.; Kolukisaoglu, H. U.; Koch, G.; Wallmeroth, N.; Hecker, A.; Thurow, K.; Zell, A.; Harter, K.; Wanke, D. *PLoS One* **2013**, *8* (10), e75177.
(6) Neuman, K. C.; Nagy, A. *Nat. Methods* **2008**, *5* (6), 491−505.
(7) Hillisch, A.; Lorenz, M.; Diekmann, S. *Curr. Opin. Struct. Biol.* **2001**, *11* (2), 201−7.
(8) Svoboda, K.; Block, S. M. *Cell* **1994**, *77* (5), 773−84.
(9) Wang, M. D.; Schnitzer, M. J.; Yin, H.; Landick, R.; Gelles, J.; Block, S. M. *Science* **1998**, *282* (5390), 902−7.
(10) Harada, Y.; Ohara, O.; Takatsuki, A.; Itoh, H.; Shimamoto, N.; Kinosita, K., Jr. *Nature* **2001**, *409* (6816), 113−5.
(11) Sun, B.; Johnson, D. S.; Patel, G.; Smith, B. Y.; Pandey, M.; Patel, S. S.; Wang, M. D. *Nature* **2011**, *478* (7367), 132−5.
(12) Allison, D. P.; Kerper, P. S.; Doktycz, M. J.; Spain, J. A.; Modrich, P.; Larimer, F. W.; Thundat, T.; Warmack, R. J. *Proc. Natl. Acad. Sci. U. S. A.* **1996**, *93* (17), 8826−9.
(13) Hornblower, B.; Coombs, A.; Whitaker, R. D.; Kolomeisky, A.; Picone, S. J.; Meller, A.; Akeson, M. *Nat. Methods* **2007**, *4* (4), 315−7.
(14) Dorvel, B.; Sigalov, G.; Zhao, Q.; Comer, J.; Dimitrov, V.; Mirsaidov, U.; Aksimentiev, A.; Timp, G. *Nucleic Acids Res.* **2009**, *37* (12), 4170−9.
(15) Hall, A. R.; van Dorp, S.; Lemay, S. G.; Dekker, C. *Nano Lett.* **2009**, *9* (12), 4441−4445.
(16) Smeets, R. M.; Kowalczyk, S. W.; Hall, A. R.; Dekker, N. H.; Dekker, C. *Nano Lett.* **2009**, *9* (9), 3089−96.
(17) Kowalczyk, S. W.; Hall, A. R.; Dekker, C. *Nano Lett.* **2010**, *10* (1), 324−8.
(18) Sischka, A.; Spiering, A.; Khaksar, M.; Laxa, M.; Konig, J.; Dietz, K. J.; Anselmetti, D. *J. Phys.: Condens. Matter* **2010**, *22* (45), 454121.
(19) Spiering, A.; Getfert, S.; Sischka, A.; Reimann, P.; Anselmetti, D. *Nano Lett.* **2011**, *11* (7), 2978−82.
(20) Raillon, C.; Cousin, P.; Traversi, F.; Garcia-Cordero, E.; Hernandez, N.; Radenovic, A. *Nano Lett.* **2012**, *12* (3), 1157−64.
(21) Soni, G. V.; Dekker, C. *Nano Lett.* **2012**, *12* (6), 3180−6.
(22) Ivankin, A.; Carson, S.; Kinney, S. R.; Wanunu, M. *J. Am. Chem. Soc.* **2013**, *135* (41), 15350−2.
(23) Bell, N. A.; Keyser, U. F. *J. Am. Chem. Soc.* **2015**, *137* (5), 2035−41.
(24) Shaevitz, J. W.; Abbondanzieri, E. A.; Landick, R.; Block, S. M. *Nature* **2003**, *426* (6967), 684−7.
(25) Strick, T. R.; Croquette, V.; Bensimon, D. *Nature* **2000**, *404* (6780), 901−4.
(26) Langecker, M.; Ivankin, A.; Carson, S.; Kinney, S. R.; Simmel, F. C.; Wanunu, M. *Nano Lett.* **2015**, *15* (1), 783−90.
(27) Keyser, U. F.; Koeleman, B. N.; Van Dorp, S.; Krapf, D.; Smeets, R. M. M.; Lemay, S. G.; Dekker, N. H.; Dekker, C. *Nat. Phys.* **2006**, *2* (7), 473−477.
(28) Keyser, U. F.; van der Does, J.; Dekker, C.; Dekker, N. H. *Rev. Sci. Instrum.* **2006**, *77* (10), 105105.
(29) Trepagnier, E. H.; Radenovic, A.; Sivak, D.; Geissler, P.; Liphardt, J. *Nano Lett.* **2007**, *7* (9), 2824−30.
(30) van den Hout, M.; Vilfan, I. D.; Hage, S.; Dekker, N. H. *Nano Lett.* **2010**, *10* (2), 701−707.

DOI: 10.1021/acs.nanolett.5b03264
Nano Lett. XXXX, XXX, XXX−XXX

(31) Steinbock, L. J.; Otto, O.; Chimerel, C.; Gornall, J.; Keyser, U. F. *Nano Lett.* **2010**, *10* (7), 2493−2497.
(32) Steinbock, L. J.; Bulushev, R. D.; Krishnan, S.; Raillon, C.; Radenovic, A. *ACS Nano* **2013**, *7* (12), 11255−62.
(33) Li, W.; Bell, N. A. W.; Hernandez-Ainsa, S.; Thacker, V. V.; Thackray, A. M.; Bujdoso, R.; Keyser, U. F. *ACS Nano* **2013**, *7* (5), 4129−4134.
(34) Steinbock, L. J.; Krishnan, S.; Bulushev, R. D.; Borgeaud, S.; Blokesch, M.; Feletti, L.; Radenovic, A. *Nanoscale* **2014**, *6*, 14380−87.
(35) Steinbock, L. J.; Steinbock, J. F.; Radenovic, A. *Nano Lett.* **2013**, *13* (4), 1717−23.
(36) Heerema, S. J.; Schneider, G. F.; Rozemuller, M.; Vicarelli, L.; Zandbergen, H. W.; Dekker, C. *Nanotechnology* **2015**, *26* (7), 074001.
(37) Steinbock, L. J.; Otto, O.; Skarstam, D. R.; Jahn, S.; Chimerel, C.; Gornall, J. L.; Keyser, U. F. *J. Phys.: Condens. Matter* **2010**, *22* (45), 454113.
(38) Otto, O.; Steinbock, L. J.; Wong, D. W.; Gornall, J. L.; Keyser, U. F. *Rev. Sci. Instrum.* **2011**, *82* (8), 086102.
(39) Rohrbach, A. *Phys. Rev. Lett.* **2005**, *95* (16), 168102.
(40) Otto, O.; Sturm, S.; Laohakunakorn, N.; Keyser, U. F.; Kroy, K. *Nat. Commun.* **2013**, *4*, 1780.
(41) Laohakunakorn, N.; Gollnick, B.; Moreno-Herrero, F.; Aarts, D. G.; Dullens, R. P.; Ghosal, S.; Keyser, U. F. *Nano Lett.* **2013**, *13* (11), 5141−6.
(42) Bulushev, R. D.; Steinbock, L. J.; Khlybov, S.; Steinbock, J. F.; Keyser, U. F.; Radenovic, A. *Nano Lett.* **2014**, *14* (11), 6606−13.
(43) Laohakunakorn, N.; Keyser, U. F. *Nanotechnology* **2015**, *26* (27), 275202.
(44) Laohakunakorn, N.; Thacker, V. V.; Muthukumar, M.; Keyser, U. F. *Nano Lett.* **2015**, *15* (1), 695−702.
(45) van Dorp, S.; Keyser, U. F.; Dekker, N. H.; Dekker, C.; Lemay, S. G. *Nat. Phys.* **2009**, *5* (5), 347−351.
(46) Aiken, C.; Gumport, R. I. *Nucleic Acids Res.* **1988**, *16* (16), 7901−16.
(47) Rivetti, C.; Guthold, M.; Bustamante, C. *EMBO J.* **1999**, *18* (16), 4464−75.
(48) Loizos, N.; Darst, S. A. *J. Biol. Chem.* **1999**, *274* (33), 23378−86.
(49) Halford, S. E.; Johnson, N. P.; Grinsted, J. *Biochem. J.* **1980**, *191* (2), 581−92.
(50) Halford, S. E.; Johnson, N. P. *Biochem. J.* **1980**, *191* (2), 593−604.
(51) Sidorova, N. Y.; Rau, D. C. *Proc. Natl. Acad. Sci. U. S. A.* **1996**, *93* (22), 12272−7.
(52) Robinson, C. R.; Sligar, S. G. *Proc. Natl. Acad. Sci. U. S. A.* **1998**, *95* (5), 2186−91.
(53) Walker, G. C. *Annu. Rev. Biochem.* **1985**, *54*, 425−57.
(54) Rice, K. P.; Eggler, A. L.; Sung, P.; Cox, M. M. *J. Biol. Chem.* **2001**, *276* (42), 38570−81.
(55) Takahashi, M.; Norden, B. *Adv. Biophys.* **1994**, *30*, 1−35.
(56) Levin, J. R.; Krummel, B.; Chamberlin, M. J. *J. Mol. Biol.* **1987**, *196* (1), 85−100.
(57) Severinov, K.; Goldfarb, A. *J. Biol. Chem.* **1994**, *269* (50), 31701−5.
(58) Galla, L.; Meyer, A. J.; Spiering, A.; Sischka, A.; Mayer, M.; Hall, A. R.; Reimann, P.; Anselmetti, D. *Nano Lett.* **2014**, *14* (7), 4176−82.
(59) Sischka, A.; Galla, L.; Meyer, A. J.; Spiering, A.; Knust, S.; Mayer, M.; Hall, A. R.; Beyer, A.; Reimann, P.; Golzhauser, A.; Anselmetti, D. *Analyst* **2015**, *140* (14), 4843−7.
(60) Smeets, R. M. M.; Keyser, U. F.; Krapf, D.; Wu, M. Y.; Dekker, N. H.; Dekker, C. *Nano Lett.* **2006**, *6* (1), 89−95.
(61) Willmott, G. R.; Parry, B. E. T. *J. Appl. Phys.* **2011**, *109* (9), 094307.
(62) Kim, S. C.; Kannam, S. K.; Harrer, S.; Downton, M. T.; Moore, S.; Wagner, J. M. *Physical review. E, Statistical, nonlinear, and soft matter physics* **2014**, *89* (4), 042702.
(63) Kesselheim, S.; Muller, W.; Holm, C. *Phys. Rev. Lett.* **2014**, *112* (1), 018101.
(64) Squires, A.; Atas, E.; Meller, A. *Sci. Rep.* **2015**, *5*, 11643.
(65) Firnkes, M.; Pedone, D.; Knezevic, J.; Doblinger, M.; Rant, U. *Nano Lett.* **2010**, *10* (6), 2162−7.
(66) Yusko, E. C.; Johnson, J. M.; Majd, S.; Prangkio, P.; Rollings, R. C.; Li, J.; Yang, J.; Mayer, M. *Nat. Nanotechnol.* **2011**, *6* (4), 253−60.
(67) Hernandez-Ainsa, S.; Muus, C.; Bell, N. A.; Steinbock, L. J.; Thacker, V. V.; Keyser, U. F. *Analyst* **2013**, *138* (1), 104−6.

DOI: 10.1021/acs.nanolett.5b03264
Nano Lett. XXXX, XXX, XXX−XXX